
Article:
You, Y., Ford, K.L. orcid.org/0000-0002-1080-6193, Rigelsford, J.M. et al. (1 more author) (2018) Systems analysis of a pattern reconfigurable antenna for capacity improvement of cell edge users in cellular networks. IEEE Transactions on Vehicular Technology, 67 (12). pp. 11848-11857. ISSN 0018-9545

https://doi.org/10.1109/TVT.2018.2875780

Systems Analysis of a Pattern Reconfigurable Antenna for Capacity Improvement of Cell Edge Users in Cellular Networks

Yingjie You, Kenneth Lee Ford, *Senior Member, IEEE,* Jonathan Michael Rigelsford, *Senior Member, IEEE,* and Timothy O'Farrell, *Senior Member, IEEE*

***Abstract*—An evaluation of a beam reconfigurable base station transceiver for cellular applications is presented from both a systems and antenna design perspective. The proposed technique uses an azimuth beam switching method which incorporates PIN diodes to provide a fast switching reflecting ground plane for a three sector antenna. Numerical systems analysis have been carried out on a hexagonal homogeneous cellular network to evaluate how the reconfigurable antenna can be used to trade-off the mean and cell edge capacity by reconfiguring the azimuth beamwidth. The systems analysis show that a mean cell edge improvement from 15Mbit/s to 18Mbit/s is achievable and this improvement is consistent for cell sizes ranging from 500m to 1500m. The proposed reconfigurable antenna has been designed, manufactured and characterised and the measured results are shown to be similar to simulations.**

***Index Terms*—Pattern reconfigurable antenna, cellular networks, network capacity.**

I. Introduction

ENHANCING cellular quality of service (QoS) beyond 4G is of global interest to both industry and academia where QoS may be quantified by a number of metrics including capacity, latency, energy efficiency, [1], etc. In this paper we are specifically interested in balancing network capacity in terms of an average user distributed across a sector and users distributed towards the edge of a cell in order to increase the minimum capacity available to a user. One possible solution is to use dynamic or reconfigurable antennas, [2], [3] that can adapt to user requirements or the distribution of users across a sector. Pattern reconfigurable antennas have been proposed as a possible solution capable of balancing network traffic, improving network capacity, increasing system gain and security, reducing noise, reducing traffic jamming and improving energy efficiency by altering or steering its radiation pattern, [4]–[6]. Reconfigurable antennas can provide the flexibility and freedom to the network by redirecting or widening/narrowing the beam and can shift the overloaded sector users to underutilized sectors. Also, through adjusting the beam width of the antenna, the coverage of the network has been shown to be improved [7], [8].

The authors are with the Department of Electronic and Electrical Engineering, University of Sheffield, Sheffield, UK, e-mail: l.ford@sheffield.ac.uk.

Manuscript received April 19, 2018; revised September 6, 2018; accepted October 9, 2018.

Reconfigurable antennas have been studied for many years for controlling the radiation pattern, resonant frequency and polarization. This can be achieved through changing the antenna characteristics, hence, altering the current flow on the antenna to achieve different performance, [9]. Proposed methods for achieving reconfigurability include mechanical movement, phase shifters, PIN/varactor diodes, MEMS, and active materials, [10]–[12] have been demonstrated on a range of antenna types such as dipoles, monopoles and patch antennas. Specific pattern reconfigurable antennas research has been carried out in areas such as changing the main lobe direction, changing the beam width or combining these two characteristics, [13]–[20]. Research has also been carried out combing antennas with metasurfaces including frequency selective surfaces, electromagnetic bandgap surfaces and artificial magnetic conductors to provide pattern reconfigurability, [21]–[27].

However, the benefits of utilization of reconfigurable antennas are not completely clear from the system point of view. Recent research shown in [28], [29] demonstrate the potential capabilities of pattern-reconfigurable antennas to achieve network flexibility and solve the challenges that modern cellular networks face. In [28], a pattern-reconfigurable antenna consisting of a driven dipole and a 3-D parasitic enclosure comprising of small metallic pixels interconnected by PIN diode switches is proposed, which can achieve both the azimuthal beam steering and elevation tilts. A utility-based cell and mode selection scheme is then optimized for 3GPP 5G networks by using this pattern-reconfigurable antenna. It is seen that by using this pattern diversity, both the average coverage and throughput gains can be improved by 13% and 29% compared to omni-type antenna equipped small cells. In [29], a planar reconfigurable beam steering antenna adapting its operation modes by using a driven patch antenna and pixelated metallic strips interconnected via PIN diodes above it is proposed. By jointly optimizing the reconfigurable antenna pattern modes and user spatial distribution in a 5G wireless system at access point antennas, the average system coverage and throughput can be improved by 29% and 16% concurrently against the system using legacy patch antennas for a hotspot scenario. Both of the papers are focusing on jointly optimizing the pattern reconfigurable antenna operation modes with cell selection or user spatial distribution algorithms for average coverage and throughput gains. However, very little research has been conducted on evaluating reconfigurable

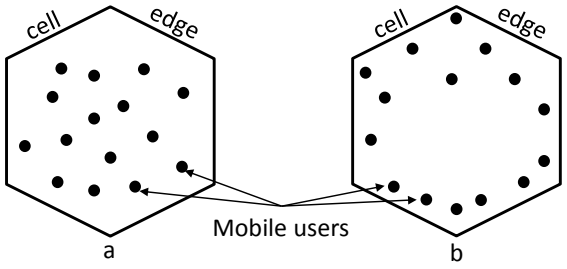

Fig. 1. User distribution within the cell, a) uniform user distribution, b) users distribute towards the edge

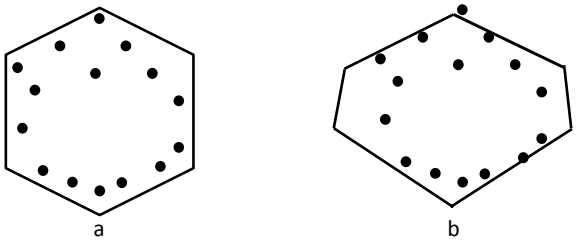

Fig. 2. Concept of how azimuth beamwidth changes cell edge position by altering between narrow a) and wide b) beamwidth

antennas in a cellular mobile systems context to enhance cell edge performance. In this paper we investigate how, within a homogeneous cellular deployment, varying the antenna beamwidth trade-offs can be made between 1) increasing the available capacity for cell edge users and 2) maximizing the average user capacity. The influence of mechanical tilt, inter site distance, path loss model and vicinity of cell edge are described. A novel reconfigurable antenna is proposed, which is capable of achieving the required system performance and a prototype antenna is demonstrated through simulations and measurements at a frequency of 1.9GHz for demonstration purposes, which is typical for cellular carrier frequencies.

II. Reconfigurable Network Concept

A. Concept assumptions

An illustration of how network users may be distributed within a hexagonal cell is given in Fig. 1. The first scenario is that users would be uniformly distributed and as such the radiation pattern should maximize the average capacity across the cell (Fig. 1a). Fig 1b shows a second scenario where users may be distributed towards the edges of the cell where significantly lower capacity is available than the average. Our motivation in this scenario is to instantaneously switch the azimuth beamwidth of the basestation antenna to a wider beamwidth, producing the situation shown in Fig. 2. The users are located in the same physical location but are now further away from the edge of the new wide beamwidth cell where the capacity may be higher. Network providers could use this concept to offer maximum average capacity or improved edge capacity to cellular users or even to reconfigure the antenna according to a scheduling policy between cell centre and cell edge users.

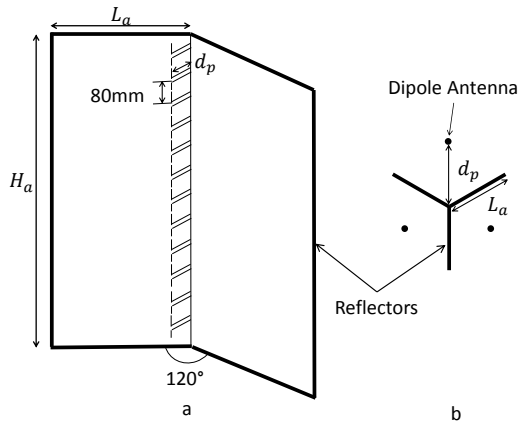

Fig. 3. Antenna model for reconfigurable azimuth beamwidth, a) side view, b) cross-section

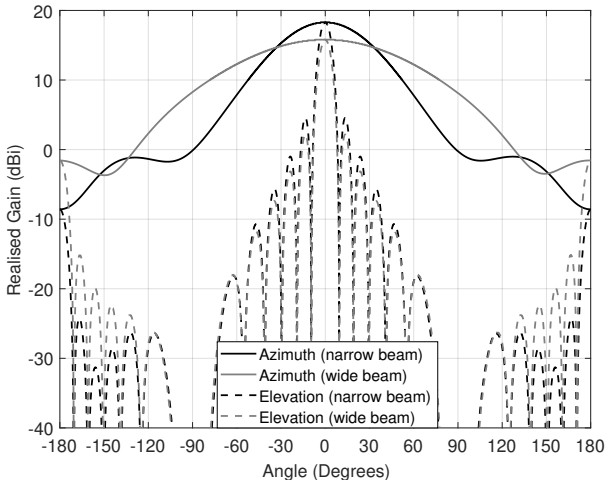

Fig. 4. Radiation pattern of reconfigurable antenna for 12 element antenna array showing the wide (110°) and narrow (60°) designs

B. Reconfigurable antenna concept

Fig. 3 shows an illustration of the proposed pattern reconfigurable antenna which consists of three radiating elements (dipoles in this case) spaced a distance, d_p, away from the centre of the base station. Three metallic reflectors of length, L_a, and height, H_a, extend from the centre of the base station with an angle of 120° between each reflector where such a configuration is suitable for a three sector cellular deployment. To provide azimuth beamwidth reconfigurability the length of the reflectors can be varied. As the reflector length, L_a, tends to zero each dipole will have an omni-directional pattern whereas for longer lengths of reflector the beamwidth will reduce to a minimum beamwidth limit. To assess the range of available beamwidths, initial antenna simulations were carried out using computer simulation software (CST) Microwave Studio, which is a 3D full wave simulator based on a finite integral technique. By changing the reflector length the azimuth beamwidth can be varied between approximately 50° and 180° where the relationship between the beamwidth and reflector length can be estimated using (1),

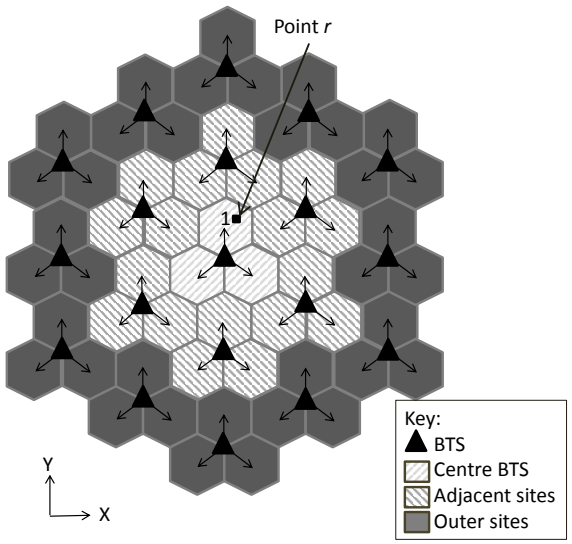

Fig. 5. Homogeneous cell deployment, including simulation observation area (denoted by hatched areas)

$$\phi_{3dB} = 170e^{-4\frac{L_a}{\lambda}} + 48, \quad (1)$$

which was found by curve fitting to the full field simulation results, where λ is the transmission wavelength.

In order to achieve an antenna gain that is commensurate with typical cellular network deployments, [30], a 12-element vertical antenna array was modelled and the corresponding azimuth and elevation radiation patterns for 60° and 110° azimuth beamwidths are shown in Fig. 4. The simulations were carried out at 1.9GHz with dimensions as follows, d_p=39.5mm, H_a=1000mm and L_a= 36.5mm and 97mm for 110° and 60°, respectively.

III. System Model

Fig. 5 illustrates a homogeneous base transceiver station (BTS) deployment made up of 19 BTS where each BTS is on a hexagonal lattice and are separated by an inter-site distance (ISD) and each BTS has three sectors fed by an antenna. Fig. 5 shows the defined observation area for the analysis, which covers the central BTS site as well as the adjacent 6 BTS sites, which is used to calculate the system performance. The observation area is discretized, using a Cartesian coordinate system where each pixel is 10m × 10m. The aim of the system model is to calculate the signal-to-interference-plus-noise-ratio (SINR) for each pixel, which in turn provides the available capacity at each pixel. The SINR and capacity data are analyzed to provide cell edge and cell mean performance for the cell denoted 1 in Fig. 5. The BTS antenna radiation patterns as shown in Fig. 4 are employed in the model where the antennas can be mechanically tilted in elevation between 0° to 15°. One of the aims of this paper is to evaluate how system performance varies depending on the size of the cellular deployment, hence, the ISD is varied from 500m to 1500m, which would represent small to large macrocell deployments. Table I provides the input parameters used in the system model, which represent typical values [31]. We are interested in urban deployments and as such the WINNER II (Urban macro — NLOS: hexagonal layout) path loss model has been employed throughout, [30]. It has been assumed that as the ISD increases the BTS antenna height, *H*, also increases and is calculated using H=ISD/45.

TABLE I
System Simulator Parameters

P	Transmit Power	40W
f	Operating frequency	1.9GHz
B	Bandwidth	20MHz
N	Number of BSs in RAN	19
M	Number of sectors in BTS	3
n_0	AWGN 1-sided PSD	4x10^{-21} W/Hz
n_{UE}	User noise figure	8dB
G_r	Receiver Antenna Gain	-1dB
L	Path Loss	WINNER II (5)
h	User antenna height	1.5m
H	Base-station Antenna Height	11-33m
ϕ_t	Antenna downtilt angle	0-15degrees
ISD	Inter-site Distance	500m-1500m

A. SINR Calculation

The center BTS is located at the origin (0,0) of a Cartesian coordinate system. We assign $(x_{n,m}, y_{n,m})$ to identify the position of the n^{th} BTS site and m^{th} sector, where the total number of cell sites, *N*, is 19 and sectors, *M*, is 3 giving 57 cells. Consider a point, *r*, in the observation area, which is denoted as position (x_r, y_r). The received power, in dB, at point *r* from the n^{th} BTS site and m^{th} sector is given by ,(2),

$$P_{n,m,r}(dB) = 10log_{10}(P) + G(\theta_{n,m} - \theta_t, \phi_{n,m}) - L_{n,r} + G_r \quad (2)$$

and the linear form is given by (3)

$$P_{n,m,r} = 10^{P_{n,m,r}(dB)/10}, \quad (3)$$

where *P* is the antenna transmitting power, $L_{n,r}$ is the path loss between the n^{th} BTS and point *r*, and G_r is the gain of the receive antenna and is assumed to be isotropic. $G(\theta_{n,m} - \theta_t, \phi_{n,m})$ is the gain of the BTS antenna for a given elevation, $\theta_{n,m}$, and azimuth, $\phi_{n,m}$, angle between the BTS and point *r* where the mechanical tilt angle of the transmitting antenna is θ_t. The gain is estimated, in dB, using (4), [32],

$$G(\theta_{n,m} - \theta_t, \phi_{n,m}) = G(\theta_{n,m} - \theta_t) + G(\phi_{n,m}). \quad (4)$$

The path loss model used is the WINNER II Dense Urban Macro NLOS model which is expressed in (5)

$$L_{n,r} = 26log_{10}(f) + 22.7 + 36.7log_{10}(d_{n,r}), \quad (5)$$

where f is the transmission frequency of the antenna (GHz), $d_{n,r}$ is the distance between the n^{th} BTS and point *r* in meters. We assume the user equipment (UE) attaches to the closest cell BTS, i.e. least path loss, since shadow and multipath fading are not considered. Thus, the received power from the 1st cell at the 1st BTS is given by (6)

$$P_{1,1,r} = max(P_{n,m,r}). \quad (6)$$

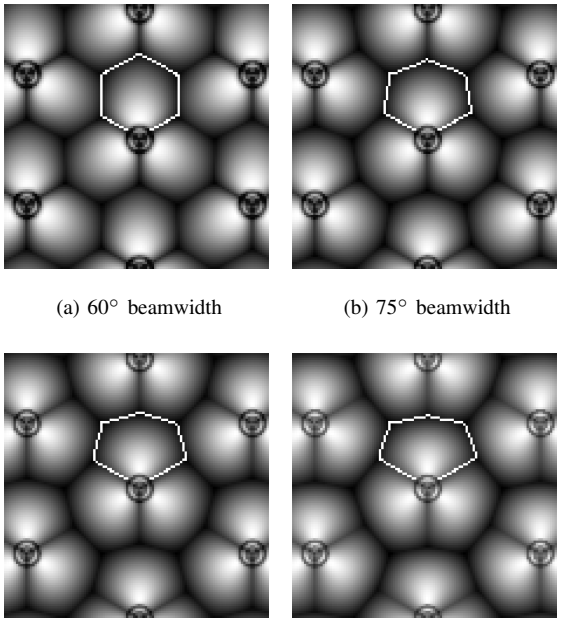

(a) 60° beamwidth (b) 75° beamwidth

(c) 90° beamwidth (d) 110° beamwidth

Fig. 6. SINR showing the detected edge of centre cell 1 for varying antenna azimuth beamwidth at tilt of 1° for ISD of 500m

The received power from the remaining sectors is treated as interference, I_r and is given by (7)

$$I_r = \sum_{n=1}^{N} \sum_{m=1}^{M} P_{n,m,r} - P_{1,1,r}. \tag{7}$$

The SINR and Shannon capacity at *r* are therefore given by (8) and (9), respectively,

$$SINR_r = \frac{P_r}{I_r + N_r} \tag{8}$$

$$C_r = B \log_2(1 + SINR_r), \tag{9}$$

where *B* is the bandwidth of the signal, N_r is the thermal noise power at the receiver given by $N_r = Bn_0n_{UE}$, n_0 is the additive white Gaussian noise power spectral density and n_{UE} is the noise figure of the receiver as defined in Table I.

B. Cell edge detection

A cell edge detection algorithm was developed to determine the physical location of the edge, which can then be used to calculate the capacity at the edge and also the cell average capacity. The central cell labelled as "1" in Fig. 5 was used to calculate the SINR gradient in the x and y directions, hence providing the local SINR minima. Example outputs of the edge detection algorithm for different antenna beamwidths are shown in Fig. 6 where the detected edge of the central cell has been superimposed onto the SINR distribution. Subsequently, the capacity of each pixel can be calculated using (9) and the cell edge and cell average capacity can are given as (10) and (11),

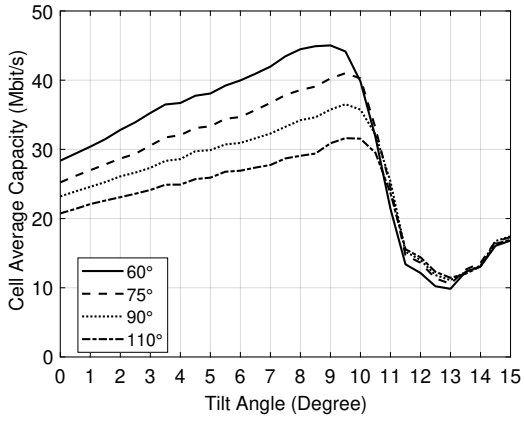

(a) Cell average capacity

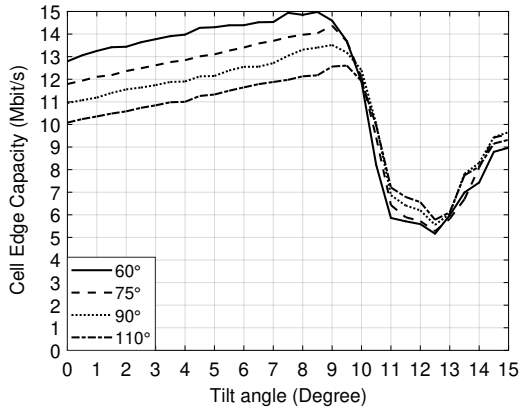

(b) Cell-edge capacity

Fig. 7. Simulated capacity for different azimuth beamwidths for ISD of 500m

$$C_a = \frac{1}{N_a} \sum_{r=1}^{N_a} C_r \tag{10}$$

$$C_e = \frac{1}{N_e} \sum_{r=1}^{N_e} C_r, \tag{11}$$

where N_a is the number of pixels in the whole cell and N_e is the number of pixels in the cell edge.

IV. Network Performance Results

A. Optimum cell beamwidth and mechanical downtilt angle

In this section, the optimum cell beamwidth and antenna downtilt angle, θ_t, are investigated by comparing a range of antenna azimuth beamwidths. The cell average capacity for beamwidths of 60°, 75°, 90° and 110° were simulated for a tilt angle range of 0° to 15° for an ISD of 500m. A comparison of the cell average capacity is given in Fig. 7a where it can be seen that the highest cell capacity occurs for a beamwidth of 60° over a tilt angle range between 0° and 10°. The optimum tilt angle for all azimuth beamwidths is between 9° and 10° and beyond this the capacity reduces as less energy is transmitted towards the edge of the cell, corresponding to the antenna beam pattern null at 13°, as observed in Fig. 4.

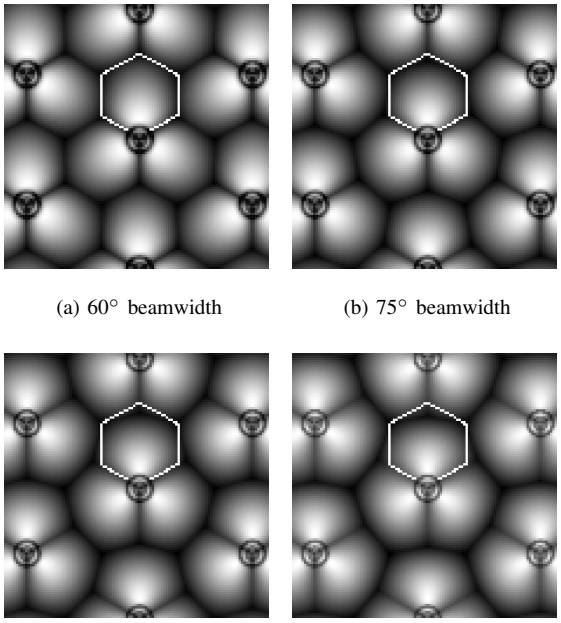

(a) 60° beamwidth (b) 75° beamwidth

(c) 90° beamwidth (d) 110° beamwidth

Fig. 8. Simulated SINR for varying azimuth beamwidth including superimposed cell-edge for the 60° case

Beyond a tilt angle of 13° the first sidelobe of the antenna radiation pattern provides more coverage to the cell-edge and hence the capacity increases. Using the previously developed cell-edge detection method, the cell-edge capacity for varying antenna beamwidth is presented in Fig. 7b, and shows that the 60° beamwidth seems to offer good performance when compared to wider antenna beamwidths.

If we consider a situation where an antenna pattern with a beamwidth of 60° is adopted these results show that we will have satisfactory performance for both whole cell and cell edge users. However, consider the case where the distribution of users is such that they are close to the cell edge and as such the network scheduling needs to serve these users. In this scenario we propose reconfiguring the antenna beamwidth to a wider radiation pattern. Then those users located near the 60° cell edge that remain in the same physical location experience a higher capacity. This scenario is evaluated in the following section.

B. Instantaneous cell edge performance assessment

To evaluate the effect of switching the antenna beamwidth to provide a higher capacity for the edge users we can consider Fig. 8 where simulated SINR are shown for varying antenna beamwidths. The assumption requires the edge users to be located near the superimposed white region in Fig. 8, which is the cell-edge for the 60° beamwidth case. The superimposed edge is then used to calculate the cell-edge capacity that users in this region might expect, using (11). Fig. 9 shows the cell average and cell-edge capacity versus tilt angle, θ_t, for a range of antenna beamwidths and ISD of 500m. Fig. 9a illustrates the trade-off in cell average capacity with a maximum of 45Mbit/s for a 60° azimuth beamwidth which reduces to 32Mbit/s for a 110° beamwidth. In contrast, the results in Fig. 9b show that the edge user capacity can be increased by 2.5Mbit/s and 3.5Mbit/s for increasing tilt angle up to approximately 9°, with deteriorating performance beyond this tilt angle. Therefore the reconfigurable antenna function would offer network providers a trade-off between cell average capacity and cell-edge capacity.

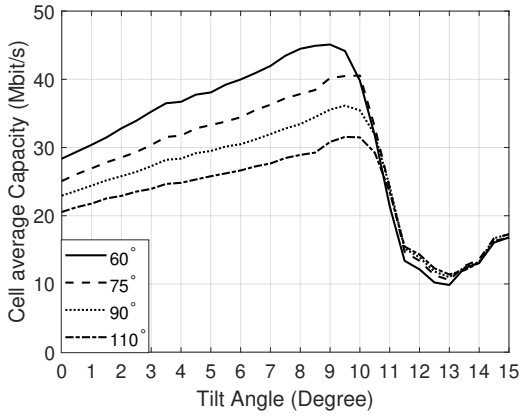

(a) Cell average capacity

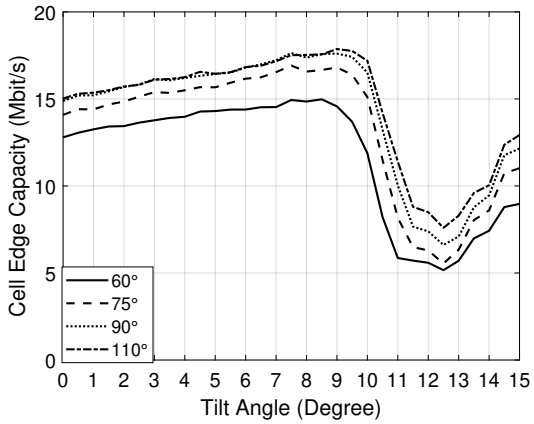

(b) Cell edge capacity

Fig. 9. Simulated capacity vs. tilt angle for antenna azimuth beamwidths of 60°, 75°, 90° and 110° when calculated using the true 60° antenna edge region and ISD of 500m

C. Impact of different path loss models

In order to evaluate the robustness of the proposed reconfigurable antenna approach against varying channel characteristics a range of alternative path loss models were investigated. For this particular study the 60° and 110° beamwidth antenna solutions were chosen. Specifically, the path loss models chosen for comparison are Winner II, Cost-Hata, and Cost 231 none-line-of-site (NLOS). The cell average capacity and the cell edge capacity are shown in Fig. 10a and Fig. 10b, respectively. The results of this study show that although there are small differences between the capacity values for different path loss models (4Mbit/s for the cell average capacity and up to 1Mbit/s for the cell edge capacity) the differences between

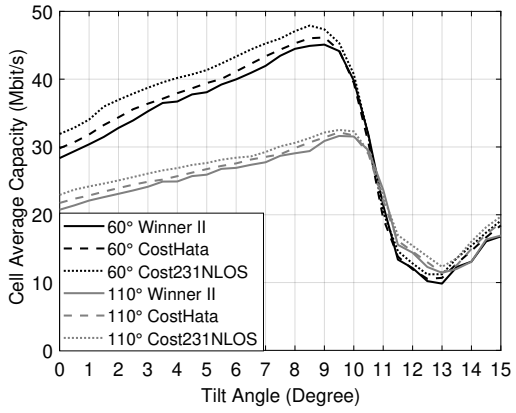

(a) Cell average capacity

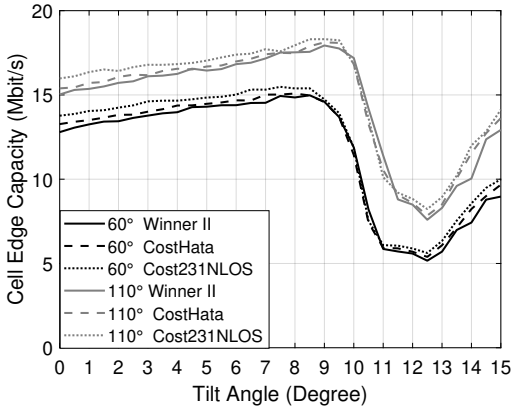

(b) Cell edge capacity

Fig. 10. Simulated capacity vs. tilt angle for 60° and superimposed on 110° azimuth beamwidth for different path loss models and ISD of 500m

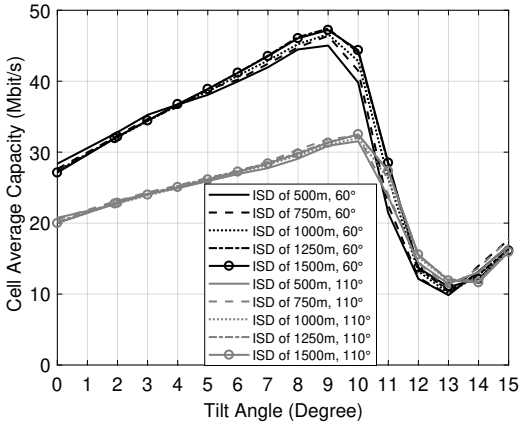

(a) Cell average capacity

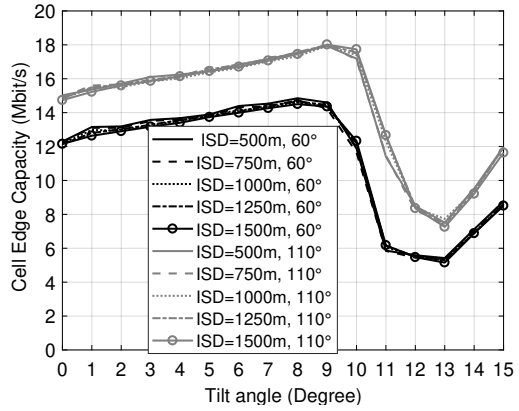

(b) Cell edge capacity

Fig. 11. Simulated capacity vs. tilt angle for 60° and superimposed on 110° azimuth beamwidth for different ISD

the 60° and 110° capacity values are not affected by the path loss models for all tilt angles.

D. Impact of ISD

This section investigates the proposed reconfigurable antenna scheme to estimate capacity for small to large area network deployments, where the ISD is varied from 500m to 1500m. It should be noted that the BTS height, *H*, is a function of the ISD where $H = \frac{ISD}{45}$ was used as a representative BTS antenna height and the simulated capacity is shown in Fig. 11. It can be seen from these results that there is a small reduction of cell average capacity as the ISD increases (Fig. 11a) for down tilt angles of approximately 9° and there is no significant change in performance for the cell edge capacity (Fig. 11b).

V. Pattern Reconfigurable Antenna

In Sections III and IV network performance simulations were based on an idealised reconfigurable antenna where the lengths of reflectors could be altered to achieve a range of azimuth beamwidths. In this section we present a novel reconfigurable azimuth controlled antenna implementation using PIN diodes, which can be reconfigured using a DC voltage, obtaining an azimuth beamwidth that can be switched between approximately 60° and 110°. The switching time of PIN diodes is several orders of magnitude less than typical modulation frames, such as 10ms for the LTE radio frame and this makes spatial scheduling feasible. The system performance of the novel antenna and idealised case is then compared. The numerical antenna simulations were carried out using CST microwave studio.

A. Array Antenna Design and Simulation

Fig. 12 shows a 12 element antenna concept and a single element for clarity. To model the whole antenna array electromagnetically, a single unit cell can be considered where periodic boundary conditions are applied to the upper and lower extremities of the unit cell. The periodic boundary conditions ensure that the effects of mutual coupling are considered without the high computational requirements of simulating a full array.

Fig. 13a shows one half of the symmetric reconfigurable reflector used to vary the antenna's azimuthal beamwidth. The reflector is 106mm wide and 79.5mm high, where the height is approximately $\lambda/2$ at the chosen design frequency of 1.9GHz and can be considered as a single unit of a periodically repeated vertical array. The reflector comprises a 1.6mm thick

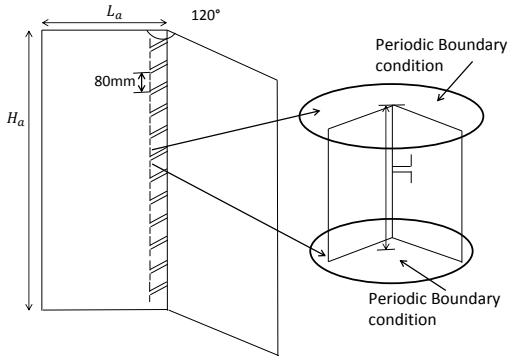

Fig. 12. 12-element pattern-reconfigurable antenna array concept including "unit cell" element

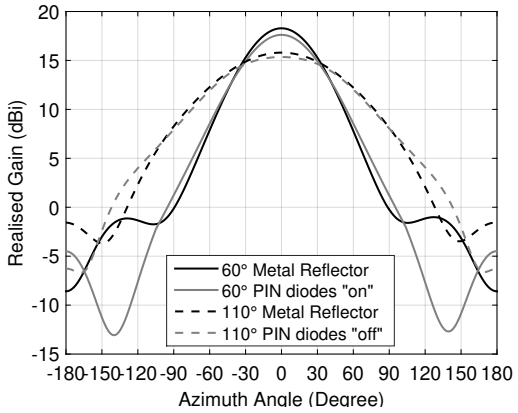

Fig. 14. Simulated azimuth radiation pattern for idealised metallic and pattern reconfigurable antennas

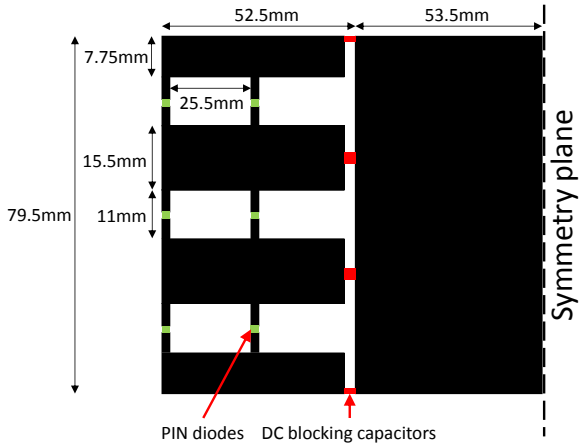

(a) Half of the reconfigurable reflector

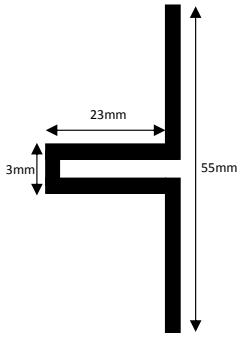

(b) Dipole antenna

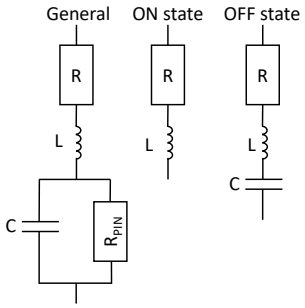

(c) PIN diode equivalent circuit model

Fig. 13. Unit cell illustration of reconfigurable reflector and dipole antenna

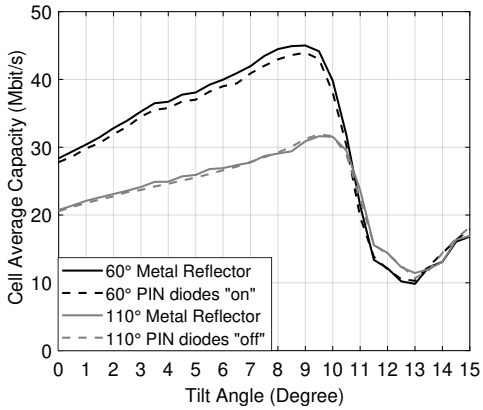

(a) Cell average capacity

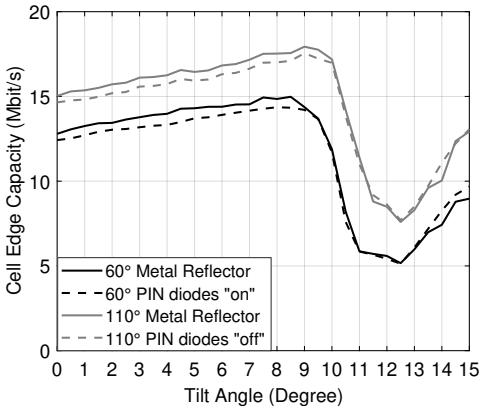

(b) Cell edge capacity

Fig. 15. Capacity vs tilt angle comparing idealised and proposed reconfigurable antennas

FR4 substrate and consists of four horizontal conducting elements connected by thin (2mm) vertical conducting strips, as illustrated in Fig. 13a where each conducting strip has a PIN diode at its center. The four horizontal elements are connected to a rectangular metallic reflector via 1nF capacitors which act as DC blocks to the bias current that is applied to the PIN diodes but act as low impedance to the RF currents. The reconfigurable reflector can be described for two modes of operation, the first being when the PIN diodes are forward biased 'ON'. When the diodes are forward biased they have a low impedance and the reflector can be approximated as a continuous conductor. This assumption can be made as the separation of the vertical conducting strips are electrically small with respect to the wavelength of the signal. The forward bias case then provides a narrow azimuth beamwidth. For the second case when the PIN diodes are not biased (or reverse biased) the diodes have a high impedance and the horizontal conducting elements can be approximated as being

semi-transparent. In this case a wide azimuth beamwidth is produced by the continuous central rectangular reflector. Two strips of diodes are needed to accurately approximate a continuous reflector where the spacing is approximately one sixth of a wavelength. The design process involved varying the lengths of the horizontal elements, the positions of the vertical strips and the width of the conducting rectangular reflector to provide an azimuth beamwidth of either 60° or 110°, which resulted in the dimensions shown in Fig. 13a.

Fig. 13b illustrates one radiating element of the reconfigurable antenna array concept. The antenna is a resonant dipole of length 55mm, which is on a 1.6mm FR4 substrate (ϵ_r=4.3, $\tan(\delta)$=0.025, not shown in the figure for clarity), the dipole includes a narrow band balun with the feed at the centre of the dipole.

To simulate the PIN diode parameters we used a simplification of a general PIN diode model which employs a series resistance, *R*, and inductance, *L*, in series with a parallel combination of capacitance, *C* and resistance, R_{PIN} as shown in Fig. 13c. The d.c bias voltage controls R_{PIN} which varies from a few ohms to several kohms depending on the device. In the on state R_{PIN} is low and effectively shorts the capacitance, *C*, leaving just the series RL. In the off state R_{PIN} is high and the capacitance, *C*, dominates which is approximated as a series RLC. This approach has been used in previous work successfully to model switchable electromagnetic structures, [33]. In this work we used the NXP BAP70-02 with parameters *R*=1Ω, *L*=0.6nH and *C*=0.12pF.

The simulated realised gain, in the azimuth plane, of the idealised and proposed novel antenna versus azimuth angle are shown in Fig. 14, where the idealised antenna is that which was shown in Fig. 4. The results show a good comparison with a maximum gain of 18dBi and 17dBi for the idealised and proposed antenna, respectively, for a beamwidth of 60°. For the 110° beamwidth case the maximum realised gain is approximately 16dBi and 15.5dBi for the idealised and proposed antennas, respectively. The differences in gain are due to uncertainties in the PIN diode model and other manufacturing tolerances.

To investigate the relevance of the design within a cellular application simulations were carried out over the 1710-1880MHz. It was found that the 'ON' state gain and beamwidth varied between 16.4-18.3dBi and 68-61°, respectively, and the 'OFF' state gain and beamwidth varied by 13.6-15.8dBi and 140-111°, respectively. It was noted that for frequencies above 2GHz the 'OFF' state beamwidth reduces as the shunt capacitance reduces the impedance of the diode.

B. System Model Performance Comparisons

In order to evaluate system performance using the reconfigurable antenna a tri-sector antenna gain pattern was simulated and embedded into the system model described in sections III and IV. Fig. 15 shows a comparison of the simulated capacity for the idealised and proposed reconfigurable antenna. Fig. 15a shows the cell average capacity where there is a 1Mbit/s difference for a 60° azimuth beamwidth and there is no significant differences for the 110° case. Fig. 15b shows a discrepancy of approximately 1Mbit/s for the idealized and proposed antennas over tilt angles between 0° and 10°. However, when comparing the differences between the two diode states a good agreement is observed.

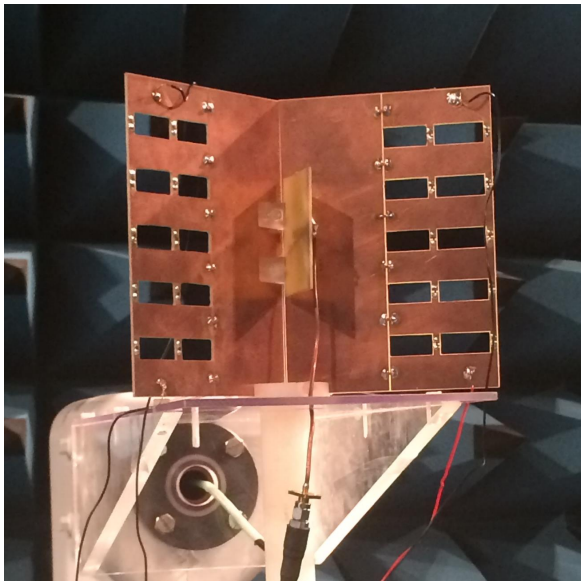

Fig. 16. Pattern reconfigurable antenna

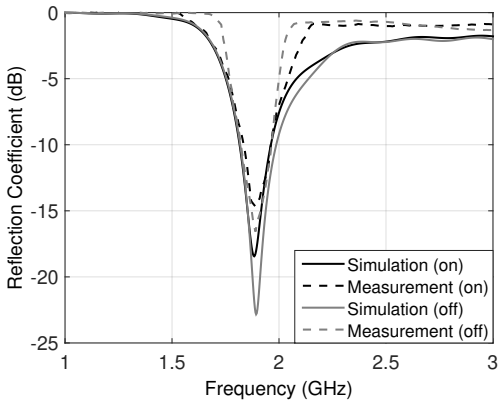

Fig. 17. Simulated and measured antenna reflection coefficient magnitude

C. Antenna measurements

To provide some confidence in the proposed reconfigurable antenna design a single antenna element was designed and manufactured using standard PCB etching techniques. The PIN diodes and DC blocking capacitors were manually soldered. A photograph of the manufactured antenna when mounted in an anechoic antenna test facility is shown in Fig. 16. The antenna input reflection coefficient was characterised for both on and off diode states and the results of this characterisation are shown in Fig. 17. It can be seen that the resonant frequency is approximately 1.9GHz for both diode states. There are some differences between the bandwidth of the measured and simulated data, which is not significant over the band of interest and is due to the uncertainty of the diode model and typical measurement uncertainties. Gain measurements and

TABLE II
COMPARISON OF NOVEL PATTERN RECONFIGURABLE ANTENNAS

Reference	Frequency range (GHz)	Gain (dBi)	Azimuth beamwidth (°)	Radiation efficiency (%)
13	2.5/5.3	5-6.5	90/100	72/88
26	1.58-2.27	5.2-7.6	81-153	88-95
28	2.47-2.9	2.7-6.4	NA	65-86
30	4.8-5.2	4.9	110	NA
31	4.9-5.1	8	40-110	81
This work		7.4-9.8	60-110	88-98

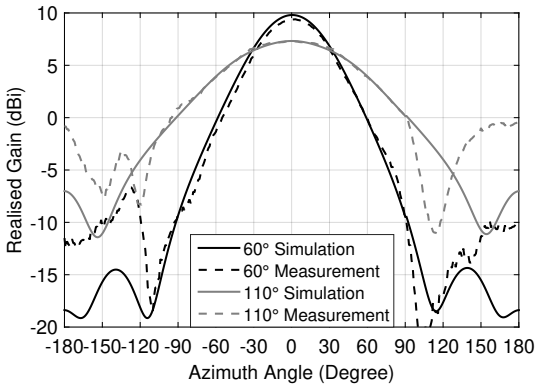

Fig. 18. Simulated and measured azimuth realised gain pattern

simulations are shown in Fig. 18 versus azimuth angle; the results show the on state gain is 9.4dBi and 9.8dBi for the measured and simulated results, respectively, and the beamwidth in both cases is approximately 59°. When the diodes are in the "off" state the gain is 7.4dBi for both the measured and simulated data with a beamwidth of approximately 110°.

VI. CONCLUSIONS

This paper has set out a concept for employing beam reconfigurable base station antennas for homogeneous cellular networks to provide instantaneous capacity improvements at cell edges when the network requires it. A novel basestation employing PIN diodes has been proposed to achieve almost instantaneous reconfigurability and simulations of a homogeneous three sector network have shown that a typical cell edge capacity increase of 20% is achievable by switching the azimuth beamwidth of the base station antenna from 60° to 110°. This capability provides the potential to trade off cell average capacity against cell edge capacity and is applicable for a range of cell sizes. Validation of the antenna concept against measurements has also been presented for a single antenna element where excellent agreement between measurements and simulations was found.

A comparison between the presented Reconfigurable antenna and other pattern reconfigurable antennas in terms of antenna working frequency, antenna gain, azimuth beamwidth and radiation efficiency is given in Table II. It is clear the proposed antenna has a higher antenna radiation efficiency and reasonable antenna gain. Also, its simple geometry makes it easy to implement in the base station and extended to any number of antenna array for current and future communication systems.

REFERENCES

[1] J. He, P. Loskot, T. O'Farrell, V. Friderikos, S. Armour, and J. Thompson, "Energy efficient architectures and techniques for green radio access networks," in *2010 5th International ICST Conference on Communications and Networking in China*, Aug 2010, pp. 1–6.

[2] S. W. O'Malley and L. L. Peterson, "A dynamic network architecture," *ACM Transactions on Computer Systems (TOCS)*, vol. 10, no. 2, pp. 110–143, 1992.

[3] D. Niyato and E. Hossain, "Dynamics of network selection in heterogeneous wireless networks: an evolutionary game approach," *Vehicular Technology, IEEE Transactions on*, vol. 58, no. 4, pp. 2008–2017, 2009.

[4] D. Jiawei, L. Yongxiang, and Z. Biao, "A survey on radiation pattern reconfigurable antennas," in *Wireless Communications, Networking and Mobile Computing (WiCOM), 7th International Conference on*. IEEE, 2011, Conference Proceedings, pp. 1–4.

[5] V. Navda, A. P. Subramanian, K. Dhanasekaran, A. Timm-Giel, and S. Das, "Mobisteer: using steerable beam directional antenna for vehicular network access," in *Proceedings of the 5th international conference on Mobile systems, applications and services*. ACM, 2007, Conference Proceedings, pp. 192–205.

[6] W. Guo, J. M. Rigelsford, K. L. Ford, and T. O'Farrell, "Dynamic basestation antenna design for low energy networks," *Progress in Electromagnetics Research C*, vol. 31, pp. 153–168, 2012.

[7] R. Jain, S. Katiyar, and N. Agrawal, "Smart antenna for cellular mobile communication," *arXiv preprint arXiv:1204.1790*, 2012.

[8] Y. Zhou, R. S. Adve, and S. V. Hum, "Design and evaluation of pattern reconfigurable antennas for mimo applications," *Antennas and Propagation, IEEE Transactions on*, vol. 62, no. 3, pp. 1084–1092, 2014.

[9] J. Bernhard, *Reconfigurable Antennas*. Morgan and Claypool, 2007.

[10] C. G. Christodoulou, Y. Tawk, S. Lane, and S. R. Erwin, "Reconfigurable antennas for wireless and space applications," *Proceedings of the IEEE*, vol. 100, no. 7, pp. 2250–2261, 2012.

[11] W. Kang and K. Kim, "A radiation pattern-reconfigurable antenna for wireless communications," in *Antennas and Propagation (APSURSI), IEEE International Symposium on*. IEEE, 2011, Conference Proceedings, pp. 1545–1548.

[12] Z. Jiajie, W. Anguo, and W. Peng, "A survey on reconfigurable antennas," in *Microwave and Millimeter Wave Technology. ICMMT 2008. International Conference on*, vol. 3. IEEE, 2008, Conference Proceedings, pp. 1156–1159.

[13] W. S. Kang, J. Park, and Y. J. Yoon, "Simple reconfigurable antenna with radiation pattern," *Electronics Letters*, vol. 44, no. 3, pp. 182–183, 2008.

[14] I. Ben Trad, J. M. Floc'h, H. Rmili, M. Drissi, and F. Choubani, "A planar reconfigurable radiation pattern dipole antenna with reflectors and directors for wireless communication applications," *International Journal of Antennas and Propagation*, vol. 2014, p. 10, 2014. [Online]. Available: http://dx.doi.org/10.1155/2014/593259

[15] S.-H. Chen, J.-S. Row, and K.-L. Wong, "Reconfigurable square-ring patch antenna with pattern diversity," *Antennas and Propagation, IEEE Transactions on*, vol. 55, no. 2, pp. 472–475, 2007.

[16] L. Petit, L. Dussopt, and J.-M. Laheurte, "Mems-switched parasitic-antenna array for radiation pattern diversity," *Antennas and Propagation, IEEE Transactions on*, vol. 54, no. 9, pp. 2624–2631, 2006.

[17] S. Nikolaou, G. E. Ponchak, J. Papapolymerou, and M. M. Tentzeris, "Design and development of an annular slot antenna (asa) with a reconfigurable radiation pattern," in *Microwave Conference Proceedings. APMC 2005. Asia-Pacific Conference Proceedings*, vol. 5. IEEE, 2005, Conference Proceedings, p. 3 pp.

[18] L. Ge and K. M. Luk, "Beamwidth reconfigurable magneto-electric dipole antenna based on tunable strip grating reflector," *IEEE Access*, vol. 4, pp. 7039–7045, 2016.

[19] L. Ge and K. Luk, "Linearly polarized and dual-polarized magneto-electric dipole antennas with reconfigurable beamwidth in the h-plane," *IEEE Transactions on Antennas and Propagation*, vol. 64, no. 2, pp. 423–431, Feb 2016.

[20] J. Ren, X. Yang, J. Yin, and Y. Yin, "A novel antenna with reconfigurable patterns lt;newline/ gt;using h-shaped structures," *IEEE Antennas and Wireless Propagation Letters*, vol. 14, pp. 915–918, Dec 2015.

[21] F. Costa, A. Monorchio, S. Talarico, and F. M. Valeri, "An active high-impedance surface for low-profile tunable and steerable antennas," *Antennas and Wireless Propagation Letters, IEEE*, vol. 7, pp. 676–680, 2008.

[22] Y. Huang, L.-S. Wu, M. Tang, and J. Mao, "Design of a beam reconfigurable thz antenna with graphene-based switchable high-impedance surface," *Nanotechnology, IEEE Transactions on*, vol. 11, no. 4, pp. 836–842, 2012.

[23] A. Edalati and T. Denidni, "High-gain reconfigurable sectoral antenna using an active cylindrical fss structure," *Antennas and Propagation, IEEE Transactions on*, vol. 59, no. 7, pp. 2464–2472, 2011.

[24] V. C. Sanchez, W. E. McKinzie III, and R. E. Diaz, "Broadband antennas over electronically reconfigurable artificial magnetic conductor surfaces," 2005.

[25] Y.-L. Tsai, R.-B. Hwang, and Y.-D. Lin, "A reconfigurable beam-switching antenna base on active fss," in *Antenna Technology and Applied Electromagnetics (ANTEM), 15th International Symposium on*. IEEE, 2012, Conference Proceedings, pp. 1–4.

[26] K. Ford and J. Rigelsford, "Antenna radiation pattern control using ebg/amc surfaces for street furniture applications," in *Antennas and Propagation Society International Symposium, IEEE*. IEEE, 2007, Conference Proceedings, pp. 4076–4079.

[27] C. Gu, B. S. Izquierdo, S. Gao, J. C. Batchelor, E. A. Parker, F. Qin, G. Wei, J. Li, and J. Xu, "Dual-band electronically beam-switched antenna using slot active frequency selective surface," *IEEE Transactions on Antennas and Propagation*, vol. 65, no. 3, pp. 1393–1398, March 2017.

[28] M. A. Hossain, I. Bahceci, and B. A. Cetiner, "Parasitic layer-based radiation pattern reconfigurable antenna for 5g communications," *IEEE Transactions on Antennas and Propagation*, vol. 65, no. 12, pp. 6444–6452, Dec 2017.

[29] M. A. Towfiq, I. Bahceci, S. Blanch, J. Romeu, L. Jofre, and B. A. Cetiner, "A reconfigurable antenna with beam steering and beamwidth variability for wireless communications," *IEEE Transactions on Antennas and Propagation*, pp. 1–1, 2018.

[30] 3GPP, "Tr36.814 v9.2.0: Lte; evolved universal terrestrial radio access (e-utra); radio frequency (rf) system scenarios (release 9)," 3GPP, Technical Report, Report, 2017.

[31] ITU-R, "M.2039-3: Characteristics of terrestrial imt-2000 systems for frequency sharing/interference analyses," ITU-R, Tech. Rep., 2014.

[32] L. Thiele, T. Wirth, K. Börner, M. Olbrich, V. Jungnickel, J. Rumold, and S. Fritze, "Modeling of 3d field patterns of downtilted antennas and their impact on cellular systems," *International ITG Workshop on Smart Antennas (WSA 2009)*, 2009.

[33] G. Kiani, "Oblique incidence performance of an active square loop frequency selective surface," *IET Conference Proceedings*, pp. 239–239(1), January 2007.

Yingjie You received a degree in Telecommunications at JiangNan University (China) in 2010. She completed an MSc in Wireless Communications in 2012, and also completed her PhD in Wireless Communications at the University of Sheffield, UK in 2018. Currently, she is a solution consultant for Dassault System in Nottingham UK. Her research interests include Reconfigurable Antenna Design, Antenna Array and Mobile Network Performance Optimisation.

Lee Ford (M'07–SM'10) received the B.Eng. and Ph.D. degrees in electronic engineering from the University of Sheffield, Sheffield, U.K., in 1998 and 2003, respectively. In 2001, he joined the Advanced Technology Centre, BAE SYSTEMS, Northamptonshire, U.K., before returning to the University of Sheffield in 2005 as a Lecturer of Communications where he was promoted to Senior Lecturer in 2012. He has been an investigator on 19 major projects including 4 sponsored by the EPSRC. He has published 135 journal and conference papers. His research interests include reconfigurable antennas, miniaturized antennas, metamaterials, propagation in the built environment, and electromagnetic structures for biomedical applications. Dr. Ford currently sits on the IET Antennas and Propagation TPN executive board and is a senior member of the IEEE.

Jon Rigelsford (SM'13) received the MEng and PhD degrees in Electronic Engineering from the University of Hull, Hull, UK in 1997 and 2001 respectively. From 2000 to 2002, he worked as Senior Design Engineer at Jaybeam Limited. From late 2002, until 2014 he was a Senior Experimental Officer for the Communications Group within the Department of Electronic and Electrical Engineering, University of Sheffield, Sheffield, UK. He is now a Senior Research Fellow at the same institution. Dr Rigelsfords current research interests include RF propagation, biomedical electromagnetics, adaptive antennas, RFID and cyber security.

Tim O'Farrell (M'91) received a BSc degree in Electrical and Electronic Engineering from the University of Birmingham, UK, and the MSc and PhD degrees in Electrical and Electronic Engineering from the University of Manchester, UK. He is Chair Professor in Wireless Communications at the University of Sheffield, UK. He is an expert in wireless communication systems specialising in physical layer signal processing, radio resource management and wireless network planning. He has pioneered research on energy efficient mobile cellular communications, the mathematical modeling of CSMA based MAC protocols for WiFi, iterative block coding for wireless communication systems and spreading sequence design for CDMA wireless networks. He is an entrepreneur, being the cofounder and CTO of Supergold Communication Limited (1997-2007), a start-up that participated in the standardisation of IEEE 802.11g with the MBCK proposal. In the framework of Mobile VCE (mVCE), Professor O'Farrell was the Academic Coordinator of the Core 5 Green Radio project (2009-2012) and a leader in establishing energy efficiency as a global research field in wireless communications systems. He has managed 23 major research projects as principal investigator with a total research spend of approximately 12M. His current EPSRC project portfolio as PI includes the SERAN and FARAD projects. He has published 312 journal and conference papers, book chapters, patents and technical reports; and has participated in standards, consultancy and expert witness activities within the wireless sector. Currently, Professor OFarrell is leading the UK Research Strategy Community Organisation in Communications, Mobile Computing and Networking within the EPSRC portfolio (www.commnet.ac.uk). Professor O'Farrell is a Director of the mVCE, a Chartered Engineer, an IET member and an IEEE senior member.